The 1st International Electronic Conference on Crystals (IECC 2018), 21–31 May 2018

IECC 2018

Tetramer compound of manganese ions with mixed valence [Mn^{II} $Mn_2^{III}Mn^{IV}$] and its spatial, electronic, magnetic and theoretical studies.

Cándida Pastor Ramírez, Sylvain Bernès, Rafael Zamorano Ulloa, Daniel Ramírez-Rosales, Hugo Vázquez Lima, Yasmi Reyes-Ortega, Samuel Hernández-Anzaldo

Introduction

Examples of Single Molecule Magnet (SMM)

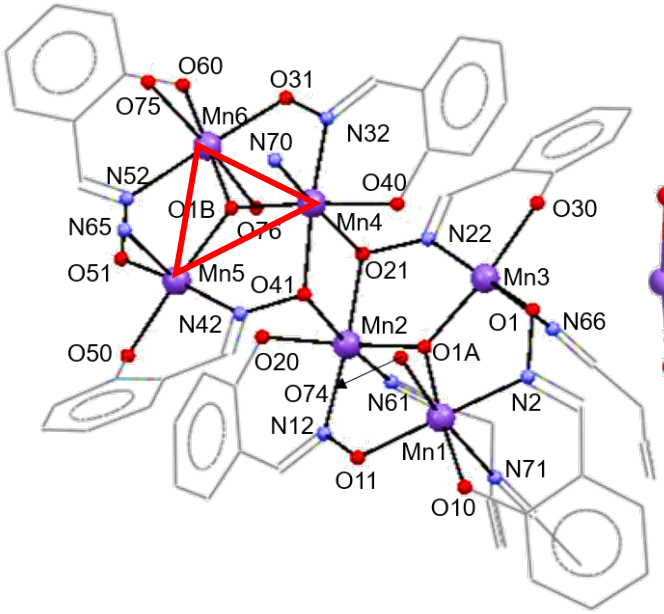

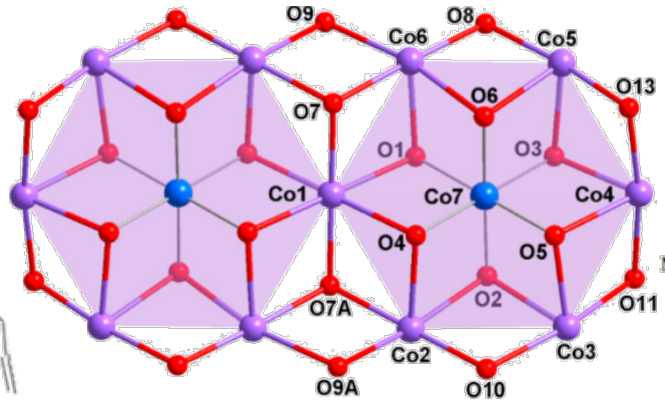

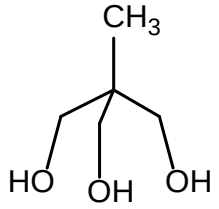

H_3thme

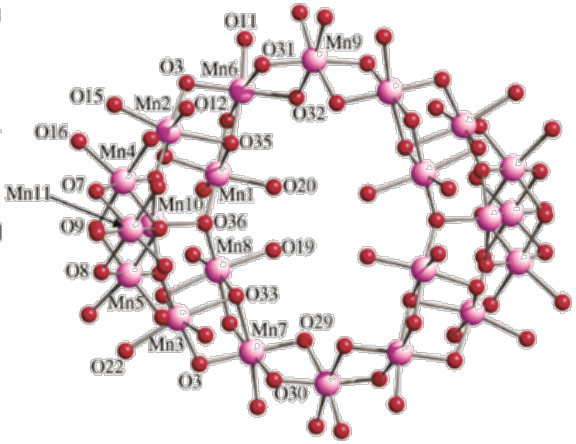

These materials (SMM)
could be used in high density information storage devices

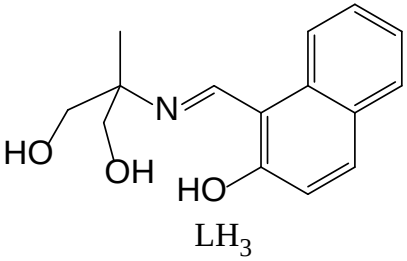

LH_3

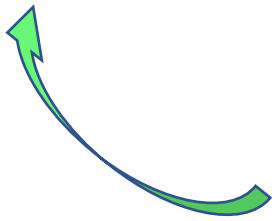

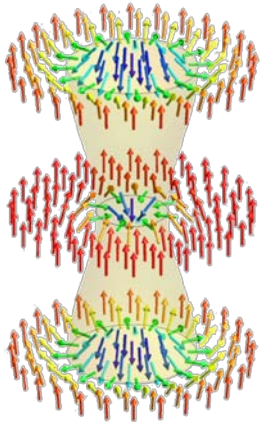

Spintronics

Brechin, E. **2005**. Murugesu *et al.,* **2004**. Reyes, Y. y Baca, E., **2016**. Leng, J. *et al.,* **2014**. Manoli, M. *et al.,* **2008**. Canaj, A. *et al*., **2015**.

Methodology and Results

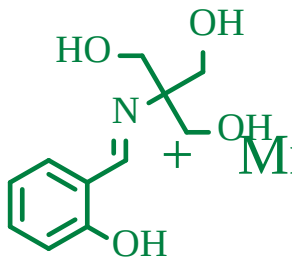

H_4L + $Mn(NO_3)_2{*}4H_2O$ + 7 NEt_3

pH ≈ 8
T. a., 1 h
Stirring
$MeOH/H_2O$

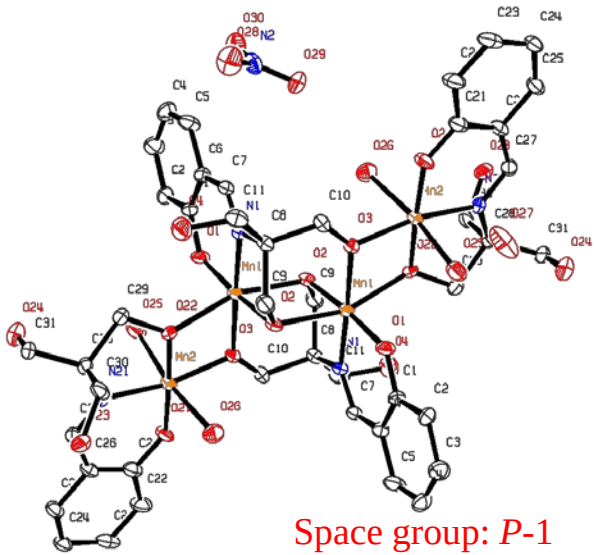

Compound	Desc. Temp. (°C)	Solubility	Yield
1 $Mn^{2+,\ 3+\ y\ 4+}$	215	MeOH, EtOH, DMSO DMF y H_2O	85%

Space group: *P*-1
V = 1428.4(7) Å^3
R-Factor (%) = 12.43
a = 10.757(3) Å
b = 11.687(3) Å
c = 13.328(4) Å
α = 98.72(2)°
β = 110.37(2)°
γ = 108.08(2)°

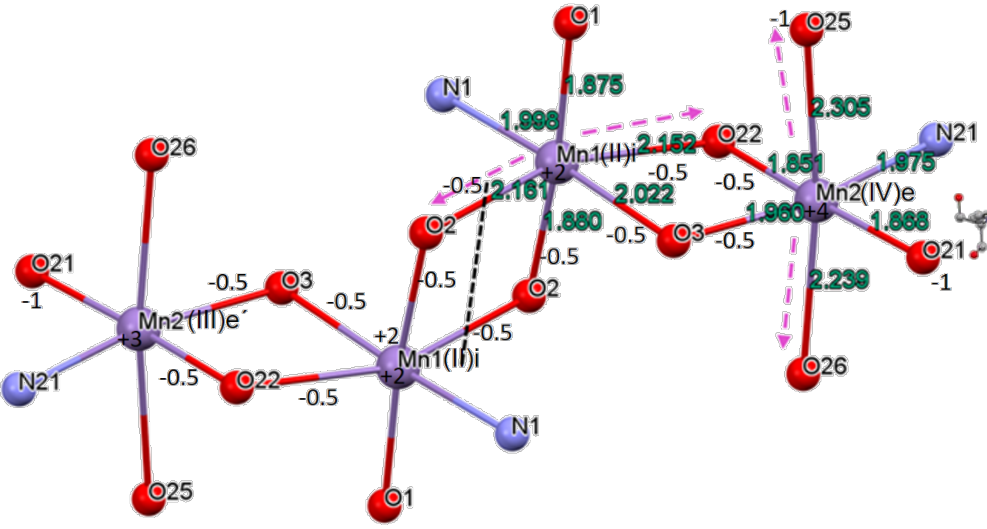

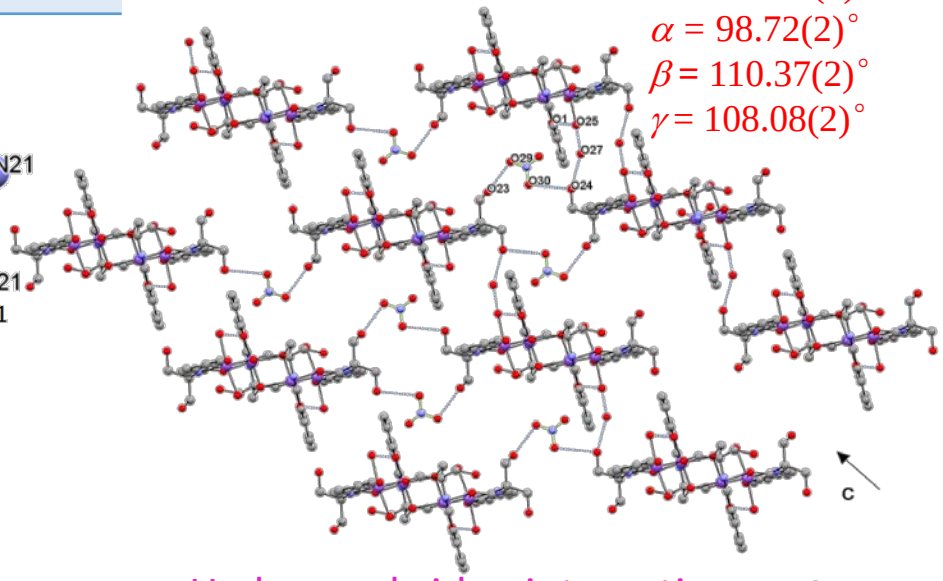

Hydrogen bridge interactions

Canaj, A. *et al*., **2015**. Cungen, Z. *et al*., **2000**. Demazeau, G. *Z*. **2010**.

Results

Experimental and theoretical Infrarred

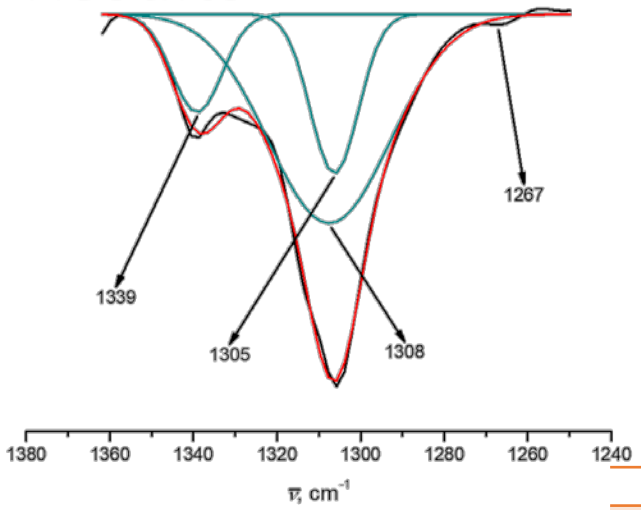

Compound	C–O Mn(II)i	C–O Mn(III)e´ Mn(II)i Mn(IV)e	C–O Mn(II)i´	C–O Mn(IV)e Mn(II)i Mn(II)i	Mn–N and / or Mn–O
1-experimental	1384	1338.59	1305.87	1290.37	447/1.45
1- theoretical calculations	1370	1340	1306	1295	

Geometric parameters of the first coordination sphere of Mn in the models optimized with B3LYP/6-31g(d)/LANL2DZ. Values in Å.

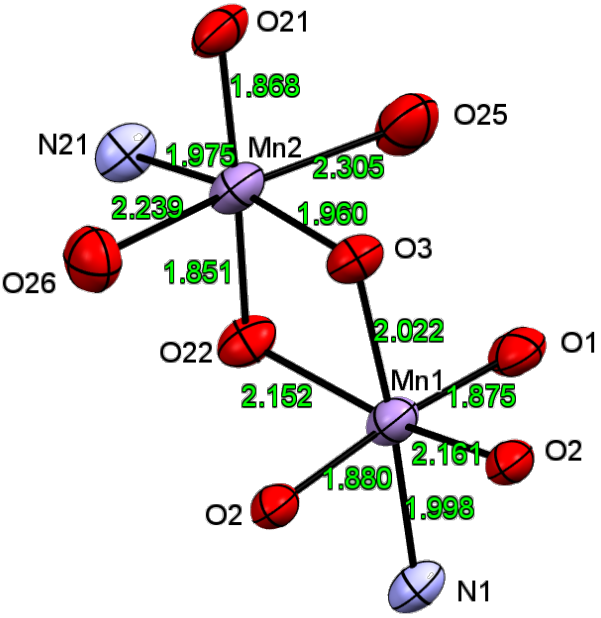

		Crystal	1	2	3	4	5	6a*	6b*
Outer	Mn-N	1.976(12)	1.960	1.936	2.000	1.948	1.973	1.990	1.974
	$Mn-O_{Ph}$	1.868(10)	1.838	1.816	1.880	1.823	1.835	1.843	1.858
	$Mn-O_{CH2\ A}$	1.960(9)	1.899	1.847	1.886	1.893	1.873	1.877	1.895
	$Mn-O_{CH2\ C1}$	1.976(12)	1.972	1.917	1.869	1.928	2.011	1.891	1.963
	$Mn-O_{H2O\ A}$	2.240(11)	2.348	1.977	2.452	2.147	3.750	1.938	2.273
	$Mn-O_{H2O\ B}$	2.305(12)	2.301	2.016	2.334	1.779	2.077	1.877	2.317
Inner	Mn-N	1.997(11)	2.000	1.964	2.174	1.985	2.226	2.225	2.006
	$Mn-O_{Ph}$	1.875(10)	1.869	1.843	2.096	1.857	2.214	2.095	1.850
	$Mn-O_{CH2\ B}$	1.880(10)	1.929	1.944	2.218	1.931	2.169	2.271	1.926
	$Mn-O_{CH2\ C1}$	2.023(9)	1.991	2.048	2.174	2.042	2.201	2.226	1.995
	$Mn-O_{CH2\ A}$	2.152(9)	2.205	2.241	2.181	2.198	2.200	2.161	2.188
	$Mn-O_{CH2\ C2}$	2.161(10)	2.299	2.250	2.088	2.279	2.108	2.184	2.378

Rafat, F. *et al*., **2004**. Shit S. et al., **2011**.Tanabe, Y. and Sugano, S., **1954**. Orgel, L. E., **1955**.

*Values a and b correspond to different sides since **6** has no *Ci* symmetry.

Results

RMN-^{1}H

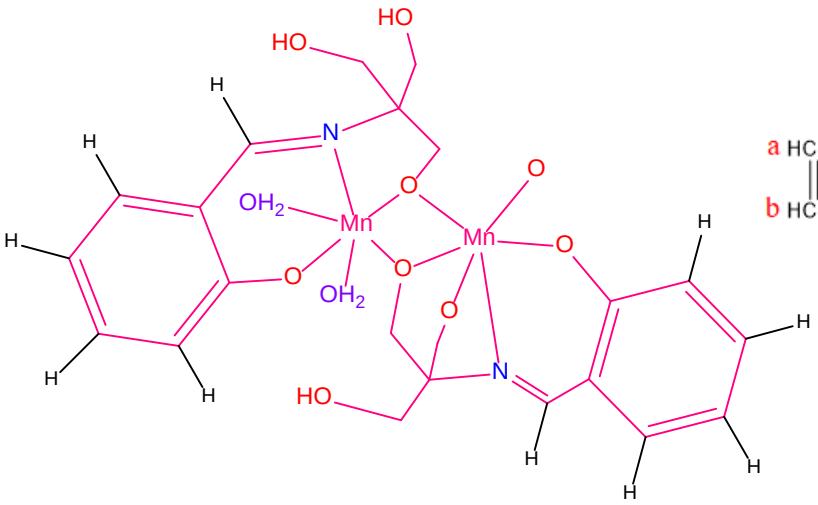

Asymmetric unit

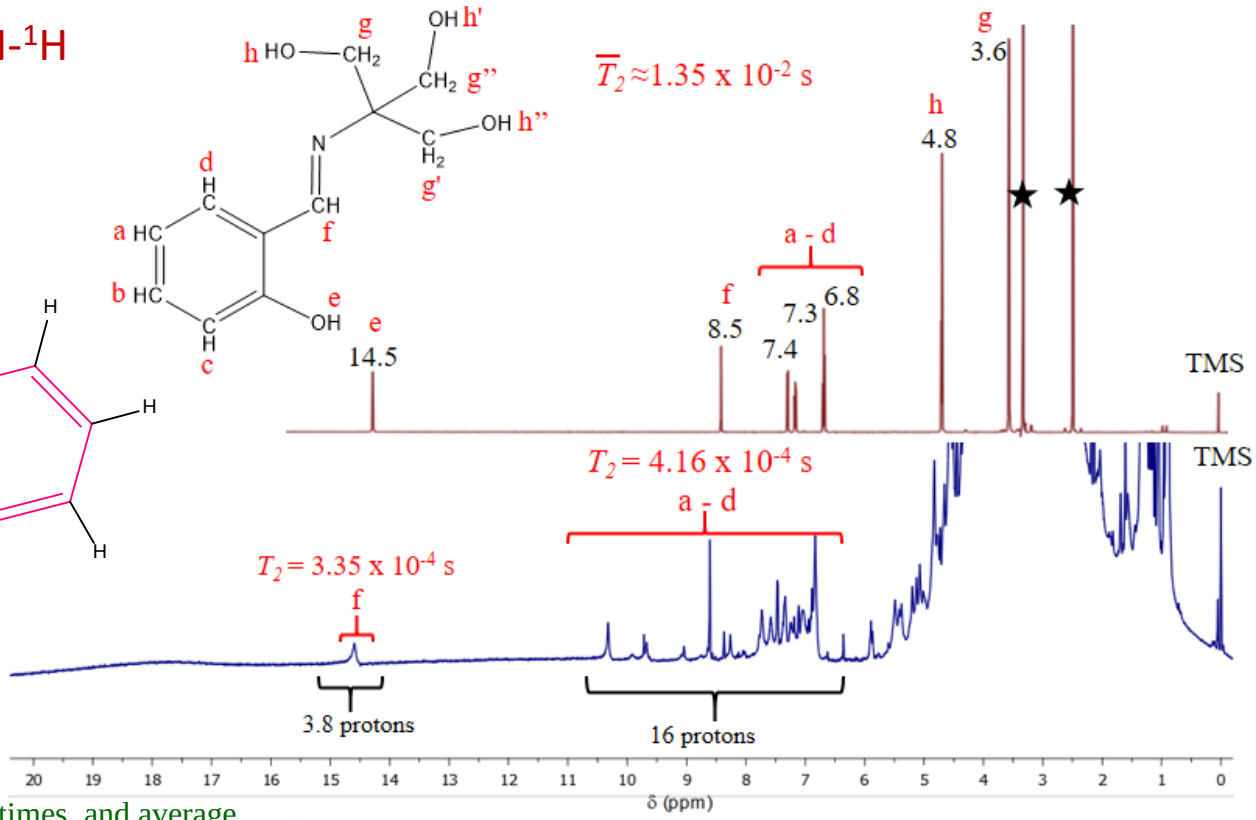

Broad lines of the chemical shifts, relaxation times, and average distances between manganese ions and protons for H_4L (blue lines) and **1** (white lines).

105 protons (approximately 4 fold to the no affected protons)

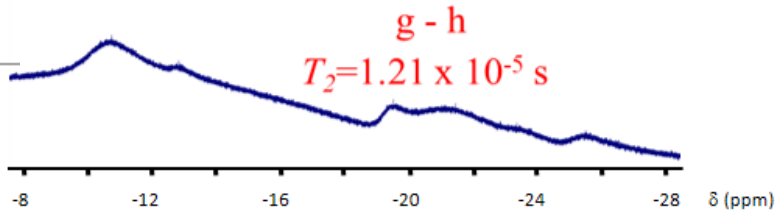

Protons	Broad signal (ppm)	T_2 (sec)	Average distance to Mn^{n+} (Å)
H_4L O–H	0.4	1.35 x 10^{-2}	n/a
H_4L aromatic	0.3	1.35 x 10^{-2}	n/a
H_4L C=N and C–H	0.1	2.25 x 10^{-2}	n/a
1, H^+ aromatic	1.5	4.16 x 10^{-4}	5.50
1, H^+ of the C=N	1.2	3.35 x 10^{-4}	3.78
1, aliphatic C–H	3	1.21 x 10^{-5}	3.06

Yuan, J. *et al.,* **2014**. Bain G. and Berry J. **2008**. Drago, R.**1992**. Kumar, D. *et al.*, **2013**. Bonadies, J. A. *et al.*, **1989**.

Results

ESR

$g = 4.48, 1.55$ for Mn(IV) high spin $s = \frac{3}{2}$, $g = 2.76$ of Mn(III) low spin $s = 1$ and $g = 1.87$ to Mn(II) low spin $s = \frac{1}{2}$.

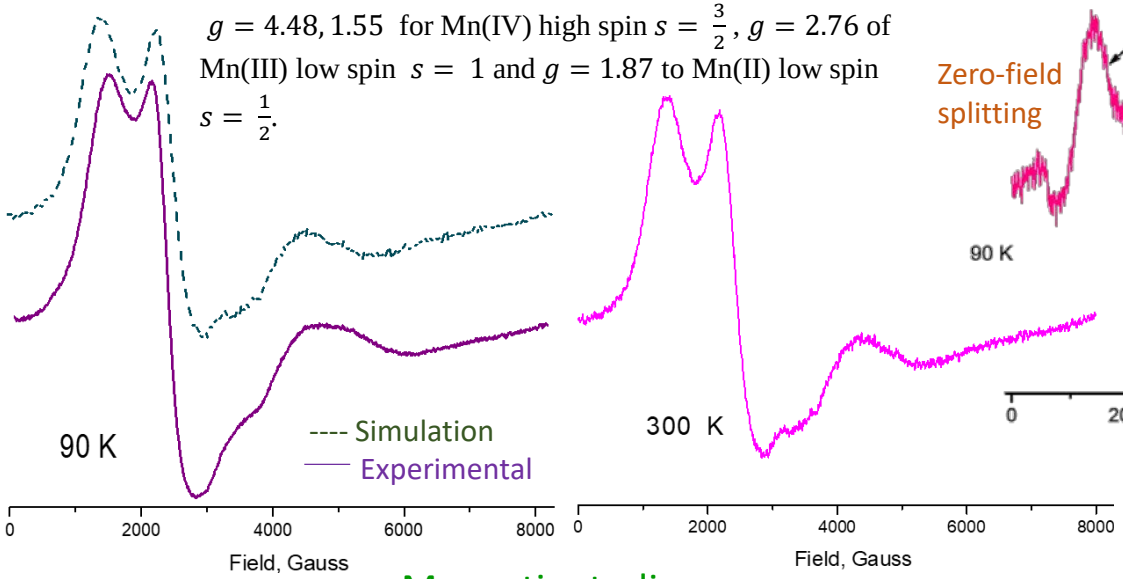

Zero-field splitting

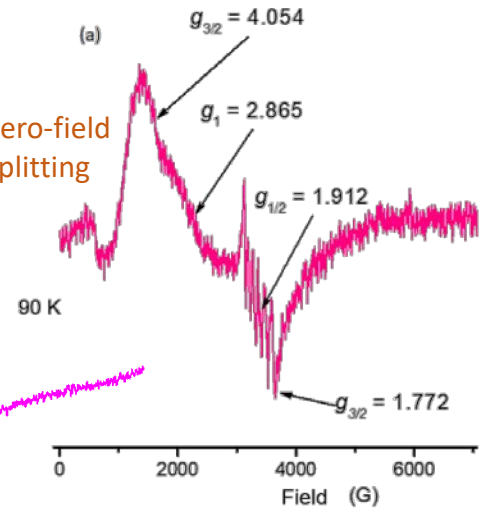

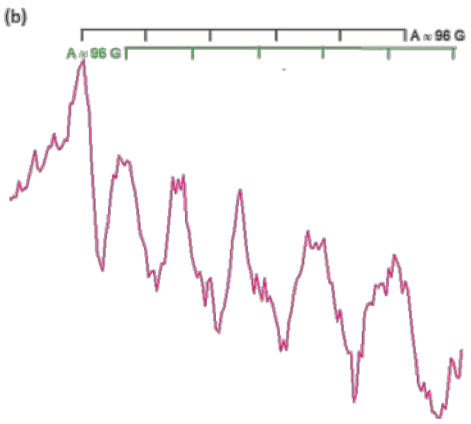

Nuclear hyperfine interaction
$I = 5/2$

Magnetic studies

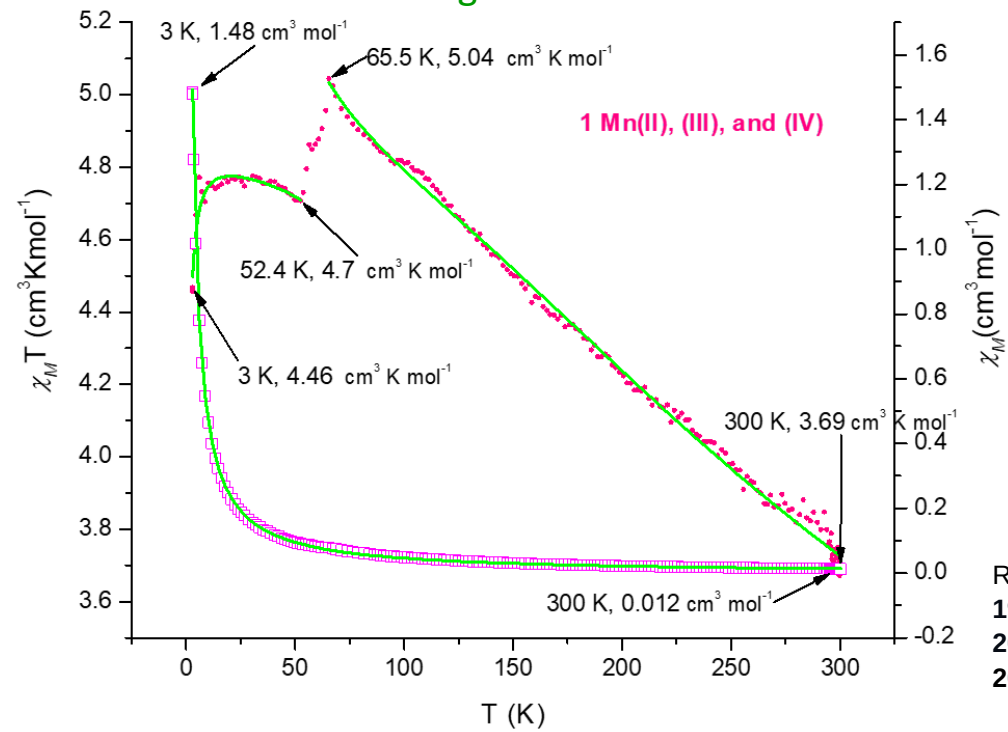

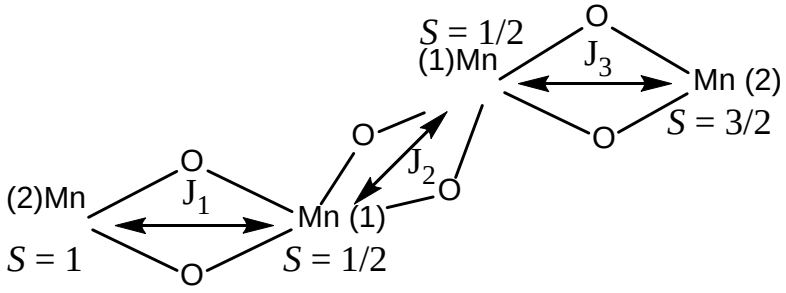

Modified Bleaney-Bowers equation

$g = 2$
$J_1 = -115.85$ cm^{-1}
$J_2 = -164.24$ cm^{-1}

Antiferromagnetic interactions

Ramírez, D. R. *et al.*, **2001**; Azamat D. V. *et al.*, **2012**. Mabbs, F. **1993**. Drago, R. **1992**. Morrish, A. , **2001**. Raptopoulou, C. *et al.*, **2013**. Milios J. C. *et al.*, **2006**. Yoo J. *et al.*, **2000**, Chen S.-Y. *et al.*, **2012**. Bleaney B. *et al.*, **1952**.

Conclusions

A different set of reaction conditions where temperature, reaction time and stoichiometry were varied consistently produced **1**. The electronic, experimental, and theoretical studies were fundamental to reconcile the crystal structure with the spectroscopic measurements obtained. The subtle structural changes caused by intramolecular electron transfer can only be established by ESR studies at different temperatures, presented as snapshots of the structural conformations. The theoretical calculations exploring oxidation and spin states on the different Manganese ions have proven to be an important tool to correlate the experimental results.

Acknowledgments

H.V.L. Acknowledges the financial support from CONACyT postdoctoral fellowship. We thank the Laboratorio Nacional de Supercomputo del Sureste (LNS), BUAP, Mexico, for providing computing resources to perform theoretical calculations. This work was financed from BUAP by Vicerrectoría de Investigación y Estudios de Posgrado Projects: REOY-NAT16-G, REOY-NAT17-G and HEAS NAT-17. Projects by Redes Temáticas PRODEP: Química de Coordinación con Aplicación al Magnetismo y Catálisis Homogénea 2015-2016 and PTC-463. CA-261-BUAP. As well as CONACyT scholarship for Cándida Pastor Ramírez.